ESMO GOOD SCIENCE BETTER MEDICINE BEST PRACTICE

IOTECH IMMUNO-ONCOLOGY AND TECHNOLOGY

ORIGINAL ARTICLE

Integrated functional and spatial profiling of tumour immune responses induced by immunotherapy: the *iPROFILER* platform

V. H. Koelzer[1], P. Herzig[2], I. Zlobec[3], V. Heinzelmann[4], D. Lardinois[5], E. Walseng[6], C. Rader[6], K. D. Mertz[7], A. Zippelius[2,8*] & D. S. Thommen[9*]

[1]Department of Pathology and Molecular Pathology, University Hospital Zurich, University of Zurich, Switzerland; [2]Department of Biomedicine, University Hospital Basel, University of Basel, Switzerland; [3]Institute of Pathology, University of Bern, Switzerland; [4]Department of Gynaecology and Obstetrics, University Hospital Basel, Switzerland; [5]Department of Surgery, University Hospital Basel, Switzerland; [6]Department of Immunology and Microbiology, The Scripps Research Institute, Jupiter, USA; [7]Institute of Pathology, Cantonal Hospital Baselland, Switzerland; [8]Medical Oncology, University Hospital Basel, Switzerland; [9]Division of Molecular Oncology and Immunology, Netherlands Cancer Institute, Amsterdam, The Netherlands

Available online 17 June 2021

Background: Cancer immunotherapy elicits functional activation and changes in immune cell distribution in cancer. Tumour heterogeneity is a reason for treatment failure but is difficult to capture in experimental settings. This proof-of-principle study describes the integrated functional and digital spatial profiling platform *iPROFILER* to capture in-situ immune activation patterns with high precision.

Materials and methods: *iPROFILER* combines an algorithm-based image analysis approach for spatial profiling with functional analyses of patient-derived tumour fragments (PDTFs). This study utilized a folate receptor 1 (FOLR1)xCD3 bispecific antibody in dual-affinity re-targeting (DART) format as a tool for inducing T-cell responses in patient tumour samples, and an in-depth investigation of the immune perturbations induced in the tumour microenvironment was performed.

Results: Ex-vivo DART stimulation induces upregulation of multiple activation markers in CD4+ and CD8+ T-cell populations and secretion of pro-inflammatory cytokines in FOLR1-positive tumour specimens. This response was reduced or absent in tissue samples that did not express FOLR1. Immunological responses were driven by a strong induction of interferon gamma (IFNγ) and IFNγ-induced chemokines suggestive of activation of cytotoxic or Th1-like T cells. Ex-vivo DART treatment led to a numerical increase in effector T cells and an upregulation of immune activation markers in the tumour microenvironment as captured by digital image analysis. Analysis of immune activation in tumour and stromal regions further supported the potential of the platform to measure local differences in cell-type-specific activation patterns.

Conclusions: *iPROFILER* effectively combines functional and spatial readouts to investigate immune responses *ex vivo* in human tumour samples.

Key words: Ex-vivo models, tumour biomarkers, immunotherapy, digital pathology, computer-assisted image processing, tumour microenvironment

INTRODUCTION

Cancer immunotherapy, particularly immune checkpoint blockade targeting the programmed death-1/programmed death ligand 1 (PD-1/PD-L1) axis, has dramatically transformed the therapeutic field in cancer.[1,2] While deep and durable responses can be observed, this is still limited to a small number of patients.[3] Combinations of antibodies blocking PD-1 and another immune checkpoint, cytotoxic T-lymphocyte-associated protein 4, have been found to increase survival,[4-6] and combination treatments with PD-1/PD-L1 are currently being tested in a large number of ongoing clinical trials.[7,8] However, many of these combinations have yielded disappointing results in phase 3 trials, underlining the need for the development of more personalized immunotherapies. To this end, a better understanding of how immunotherapies act on the tumour microenvironment (TME), as well as technologies to investigate such intratumoural immune responses, are essential.

*Correspondence to: Dr Daniela Stefanie Thommen, Division of Molecular Oncology and Immunology, Netherlands Cancer Institute, Plesmanlaan 121, 1066 CX Amsterdam, The Netherlands. Tel: +31 2 0512 7950
E-mail: d.thommen@nki.nl (D. S. Thommen).
*Correspondence to: Prof. Alfred Zippelius, Department of Biomedicine, University Hospital Basel, Hebelstrasse 20, 4031 Basel, Switzerland
E-mail: alfred.zippelius@usb.ch (A. Zippelius).

It has recently been shown that human ex-vivo systems, such as patient-derived tumour fragments (PDTFs), allow the profiling of early local immunological responses to PD-1 blockade.[9] PDTFs are approximately 1x1x1mm-sized tissue fragments processed from surgically resected tumour specimens that preserve the TME and architecture during ex-vivo culture, but can be exposed to immunotherapeutic perturbations. While measuring the reactivation of tumour-resident T cells as well as subsequent cytokine and chemokine secretion induced by PD-1 blockade reliably predicted clinical response in five cancer types, inter- and intratumoural heterogeneity in such immune reactivation was also observed.[9] This may result from distinct distribution patterns of anti-tumoural effector cells mediating the efficacy of the local anti-tumoural immune response, which cannot be captured adequately by the measurement of overall cytokine and chemokine production during ex-vivo treatment. Hence, the integration of the PDTF platform with spatial immune profiling technologies could provide a multidimensional approach to study local immune activity in the TME induced by immunotherapies.

This proof-of-concept study describes the *iPROFILER* (integrated profiling of intratumoural immune responses) platform (Figure 1), an algorithm-based image analysis approach for interrogating the cellular composition of the TME at single-cell resolution[10] combined with functional analyses in the PDTF ex-vivo system. A bispecific antibody in a dual-affinity re-targeting (DART) format was used as a tool to induce a tumour-directed T-cell response in human lung and ovarian cancer samples. The *iPROFILER* platform allowed the characterization of in-situ responses elicited by the DART by directly linking spatial tumour properties and immune activation patterns in each perturbed tumour fragment. Moreover, immunological responders and non-responders could be identified, as well as potential underlying causes for treatment resistance, highlighting the translational potential of the platform.

MATERIALS AND METHODS

PDTF cultures

PDTF cultures were performed as described previously.[9] In brief, cryopreserved PDTFs were thawed slowly, washed extensively with tumour medium [DMEM + sodium pyruvate (1 mM) + MEM non-essential AA (1x) + L-glutamine (2 mM) + penicillin/streptomycin (100 ng/ml) + 2-mercaptoethanol (50 nM) + ciproxin (1 mg/ml) + 10% fetal bovine serum] and embedded in an artificial extracellular matrix [sodium bicarbonate (Sigma, 1.1%), collagen I (BD Biosciences, 1 mg/mL), matrigel (Matrix High Concentration, Phenol Red-Free, BD Biosciences, 4 mg/mL) and tumour medium] in a flat-bottomed 96-well plate. To this end, 30 µl of matrix was added to each well and solidified at 37°C for 20-30 min. One tumour fragment was placed on top of the matrix in each well and covered with a second layer of 30 µl of matrix. PDTF cultures were topped up with tumour medium containing folate receptor 1 (FOLR1)xCD3 DART at 100 ng/mL where indicated. After 48 h of culture at 37°C, supernatants were collected and frozen immediately at −80°C for subsequent cytokine and chemokine analysis.

ngTMA generation and immunohistochemistry

Following PDTF culture, the tumour fragments were fixed in 4% formalin and embedded in paraffin according to standard protocols for a total of 36 tissue blocks (four per tumour, two untreated and two DART-treated) with one sample each. Next-generation tissue microarrays (ngTMAs)[11] were designed using digital pathology to capture and array all PDTF formalin-fixed paraffin-embedded samples on a single recipient block using an automated and digitally controlled semi-robotic tissue microarrayer with a 1.5-mm punch size (3DHISTECH Ltd, Budapest, Hungary). For visualization of immune cell infiltrates and signalling molecules, strict serial sections were cut from the finished TMA block at 4 µm for immunohistochemical staining of the following parameters: T-cell markers CD4, CD8 and FOXP3; B-cell marker CD19; proliferation markers (Ki67); markers of cell-dependent cytotoxicity (T-cell intracellular antigen 1; Granzyme B; Perforin); activation of interferon signalling [signal transducer and activator of transcription 1 (STAT1); interferon regulatory factor 1 (IRF1); IRF5]; expression of the immune checkpoint molecules PD-1 and PD-L1; visualization of tumour cells [epithelial cell adhesion molecule (EpCAM)]; and tumour cell apoptosis [apoptotic protease activation factor 1 (APAF-1), caspase 3 and caspase 9]. Binding of the primary antibodies was detected using anti-immunoglobulin-coupled horseradish peroxidase with 3,3′-diaminobenzidine (DAB, OptiView Kit, Roche Diagnostics, Ventana, catalogue no. 760-700) as substrate. Nuclear counterstaining was performed with Mayer haematoxylin. Table S3 (see online supplementary material) shows the specific staining protocols. A haematoxylin and eosin slide was generated for pathological review and assessment of tissue necrosis.

Digital image analysis

All slides were scanned at high resolution on a Pannoramic P250 slide scanner (3DHISTECH Ltd) with a 40× objective with a numerical aperture of 0.95, achieving a pixel resolution of 0.121 µm/pixel with a 12 MP camera with Xenon Flash illumination, and uploaded on to the digital image analysis platform (Indica Labs HALO, v3.1.1076.433). A board-certified pathologist reviewed all digital images. Areas with staining artefacts were excluded, and spots were segmented and annotated with the PDTF clinical metadata.

A deep neural network was trained (Simonyan and Zissermann VGG, implemented in the HALO AI™ platform[12]) to detect, annotate and measure tumour epithelium and stromal regions in each PDTF sample. In brief, html-based annotations of stromal and tumour regions were generated in the HALO graphical user interface for each ngTMA slide and each marker group of interest. A third class was introduced to capture background areas for exclusion. For all classes, a balanced representation with a minimum of 100 separate region examples was generated. Next, the VGG network implemented in HALO AI™ was trained for

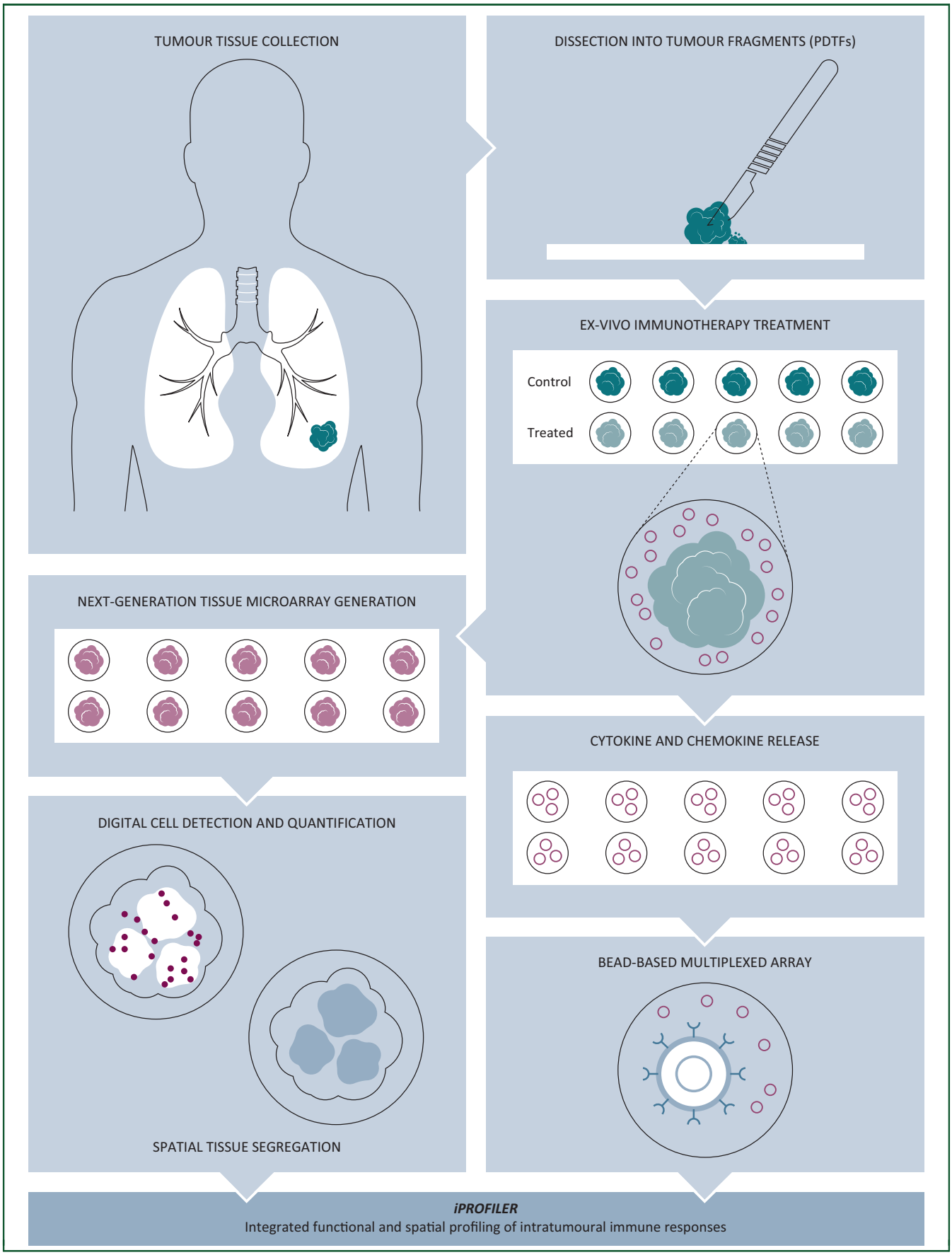

Figure 1. Integrated profiling of intratumoural immune responses — the *iPROFILER* platform.
Combination of ex-vivo culture of patient-derived tumour fragments (PDTFs) with functional and spatial analyses comparing treated and untreated samples allows for multidimensional analysis of treatment-induced immune responses at single-cell level.

the classification of tumour, stromal and background regions until convergence was achieved (cross entropy <0.1) on a NVIDIA Titan XP GPU with 12 GB of memory. Mark-up images of the predicted region labels were then generated and cross-validated against pathologist-based assessment. In the case of classification errors, additional annotations were generated, and the training and review process was repeated in an active learning process.

Nuclear density of the haematoxylin counterstain was measured following channel separation at RGB values of 57, 49 and 137, and minimum thresholds for nuclear optical density were set according to pathologist review. Nuclear segmentation was performed using a seeded watershed on the haematoxylin counterstain followed by cell/nuclear boundary detection and post processing according to pathologist-controlled cellular parameters, such as nuclear size, roundness and optical density as implemented in Indica Labs HALO, v3.1.1076.433, 'Cytonuclear' and 'Multiplex IHC' modules. Detection of the cell population of interest was controlled individually for each slide and marker. Visual overlays of the nuclear segmentation masks were generated, and quality control was performed by pathologist review. Cell detection and segmentation were optimized for detection of the cell population of interest.

Marker positivity (DAB staining) of lineage markers was detected and analysed according to pathologist-set positivity thresholds utilizing non-immune cell populations as internal controls, leading to the classification of each cell as either positive or negative. Subset analyses were performed for markers where expression intensity was of additional interest, such as interferon signalling molecules STAT1, IRF1 and IRF5. Here, the optical density of the DAB precipitate in the nuclear compartment was measured as a measure of expression intensity. For the subset analysis of interferon signalling molecules, the optical density of the DAB precipitate in the nuclear compartment was additionally measured as a measure of expression intensity. Cells were then scored as $1+$ if they exceeded the set threshold of the negative control, as $2+$ if they exceeded the set threshold of staining intensity by at least 2x, and as $3+$ if they exceeded the set threshold by at least $3\times$. Marker-positive cells were quantified separately in the tumour and stromal compartments. Areas of necrosis, staining artefacts and tissue anthracosis were excluded from analysis. Immune cell infiltrates were normalized by tissue area; for immune activation markers, the percentage of positive cells and expression intensity were recorded in each compartment. To obtain sufficient cell numbers for comparison of ex-vivo treatment effects, six PDTFs from four tumours were selected for which at least a 0.5×0.5 mm tissue area could be analysed. The reader is referred to the online supplementary material for additional details.

RESULTS

Characterization of T-cell-driven immunological responses in human cancers

To assess the immunological consequence of broad T cell activation in the TME, a bispecific antibody targeted to human CD3 and FOLR1 in a DART format was used as a tool to induce T-cell stimulation in human cancer samples. In contrast to PD-1-blocking antibodies, for which T-cell reinvigoration is limited to a small number of tumours containing tumour-specific T cells, bispecific antibodies that contain one arm specific for human CD3 and one arm directed towards a tumour antigen can broadly activate T cells by bypassing major histocompatibility complex/peptide recognition and, thus, overcome the need for antigen specificity.[13,14] Importantly, activation only occurs when the tumour antigen and the T-cell receptor are bound simultaneously. The recently described FOLR1xCD3 bispecific DART used in this study has been shown to crosslink T cells and FOLR1-expressing tumour cells efficiently *in vitro* and *in vivo*.[15] While FOLR1 shows limited expression in healthy tissues, it is highly overexpressed on the surface of cancer cells in a number of malignancies, including lung, ovarian and other solid cancers.[16] Thus, immune activation induced by the DART is limited to T cells at the tumour site.

First, the specificity of the DART was confirmed in co-culture assays by stimulating peripheral blood mononuclear cells or sorted $CD8+$ T cells from healthy donors, either in the presence or absence of the FOLR1-expressing Skov3 tumour cell line with the DART (Figure S1A,B, see online supplementary material). By performing dose titration experiments in the same experimental setting, the optimal concentration of the DART was established at 100 ng/ml (Figure S1C,D, see online supplementary material). Next, it was assessed whether the DART could also induce T-cell activation in human cancer samples, using the recently developed PDTF platform[9] (Figure 1). PDTFs from nine lung and ovarian cancer specimens (Table S1, see online supplementary material) were exposed to the DART for 48 h, and the upregulation of activation markers on $CD4+$ and $CD8+$ T cells was measured by flow cytometry (Figure 2A-C). Most tumours (7/9) showed a strong increase in multiple T-cell activation markers in both subsets upon DART treatment compared with the unstimulated control, indicating that the DART can also activate tumour-resident T cells. To investigate whether lack of FOLR1 expression and/or low immune infiltration were reasons for non- or weak response, these properties were assessed in the study samples. One of the two tumours showing no or weak T-cell activation (BS515) was negative for FOLR1, further confirming the specificity of the DART (Figure 2D; Figure S2A, see online supplementary material). The other tumour (BS295) expressed FOLR1 but showed only a minor immune infiltrate, which may explain the low level of T-cell activation induced by the DART in this sample (Figure 2E; Figure S2B, see online supplementary material).

Next, multiple cytokines and chemokines secreted by the tumours were assessed to understand whether the DART also elicits a broader immune response (Figure 3A,B). Notably, induction of IFNγ was observed in all tumours except BS515, in line with the lack of FOLR1 expression in this tumour. Interestingly, the IFNγ response could also be observed in BS295, suggesting that even a small T-cell infiltrate in a tumour may be sufficient for the DART to

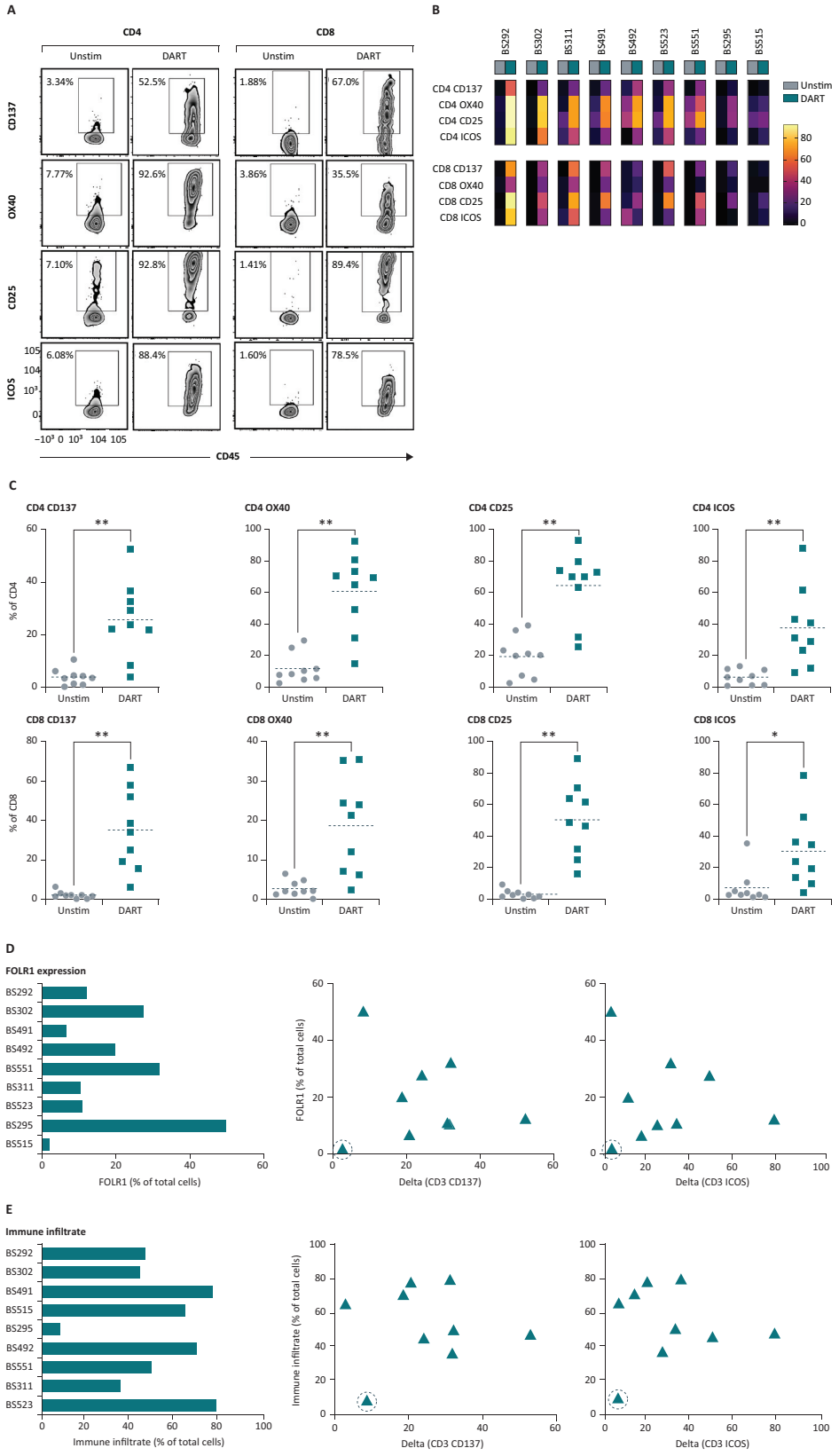

Figure 2. Folate receptor 1 (FOLR1)xCD3 DART induces T-cell activation in human lung and ovarian cancer patient-derived tumour fragments (PDTFs).
(A) Example of the flow analysis of four T-cell activation markers in CD4+ and CD8+ T cells, respectively, in unstimulated and DART-treated PDTFs. (B+C) Heatmap showing the percent expression (B) and quantification (C) of all four activation markers in CD4+ and CD8+ T cells for nine lung and ovarian cancer samples. Data represent a pooled analysis of three fragments per condition for each tumour. (D) FOLR1 expression for each tumour (left) and correlation between OX40 expression on CD4+ T cells and CD137 expression on CD8+ T cells, respectively, with FOLR1 expression (middle and right). The non-responsive tumour BS515 is indicated by the circle. (E) Immune infiltrate (% CD45+ cells within live cells) for each tumour (left) and correlation between OX40 expression on CD4+ T cells and CD137 expression on CD8+ T cells, respectively, with the immune infiltrate (middle and right). The weak responsive tumour BS295 is indicated by the circle.

https://doi.org/10.1016/j.iotech.2021.100034

induce an immune response. Secretion of the IFNγ-induced chemokines CXCL9 and CXCL10 (cluster 1) was observed in most tumours, while patterns of other cytokines and chemokines were more heterogeneous (Figure 3A,B). For instance, cluster 2 parameters consisting of some CD4 helper cytokines and the chemoattractants CCL3 and CCL4 were increased in four of the seven responding tumours, and most cluster 3 parameters remained largely unchanged in the majority of tumours. Taken together, these data underline that immunological responses upon T-cell activation by the DART are characterized by strong induction of IFNγ and IFNγ-induced chemokines that is found consistently across tumours, and may be suggestive of activation of cytotoxic or Th1-like T cells, as well as secretion of additional soluble factors that are more heterogeneous between cancers.

Development of an ngTMA and digital pathology platform for PDTF analysis

To better understand the heterogeneity of immunological responses, approaches are needed that directly link patterns of immune activation to cellular composition and architecture of patient tumour samples. To this end, the *iPROFILER* platform (Figure 1) was developed, which combines the PDTF system with an image analysis platform, thereby allowing to connect dynamic readouts to spatial information for multidimensional characterization of immune responses. As a proof-of-concept experiment, a second set of PDTFs from the seven responsive tumours were exposed to the DART as described above, but instead of performing flow cytometry after culture, the fragments were embedded in paraffin for further histological analysis. To reduce variation due to processing and staining procedures, and to enable high-throughput screening and analysis, an ngTMA was constructed as described previously[11] containing all the tumour fragments from one experiment (Figure 4A). Immunohistochemistry analysis for key cell lineage and functional markers was performed to characterize the in-situ immune response (Table S3, see online supplementary material). For each marker, a digital image quantification protocol was established, and marker-positive cells were quantified either in the full fragment or in separately annotated tumour and stroma regions as detailed in the 'Methods' section.

To test the reproducibility of the responses that were observed in the first analysis in this data set, cytokines and chemokines in the supernatant of individual PDTFs that were subjected to immunohistochemistry were assessed (Figure 4B,C; Figure S3, see online supplementary material). The response patterns to the DART were similar as observed in the experiment before, with strong induction of IFNγ in all PDTFs and more variable patterns in the secretion of other cytokines and chemokines. The average change in single parameters was comparable between the two cohorts (Figure 4D), supporting the robustness of the functional readout.

To gain better understanding of changes in the immune composition induced by the DART, CD8+, CD4+ and FOXP3+ T cells as well as CD19+ B cells in the PDTFs were quantified digitally. Changes in the tissue, such as a tendency towards increased background staining, reduced nuclear morphology, focal tissue necrosis or tissue loss, which led to the drop-out of some measurements [33/532 (6.2%) measurements], could generally be controlled by careful optimization of the image analysis protocols (Figure S4A-C, see online supplementary material). Ex-vivo treatment with the DART increased the number of T cells compared with B cells, which was significant for CD4+ T cells and showed a trend in both CD8+ and FoxP3+ T cells (Figure 4E,F). As PDTFs contain only the intratumoural T-cell compartment, this increase was suggestive of induction of local T-cell proliferation by the DART. To understand whether the increased secretion of cytokines and chemokines upon DART treatment simply reflects these higher CD4+ and CD8+ T-cell numbers in PDTFs, Spearman correlations between the changes in each soluble factor and in CD4+ and CD8+ T-cell numbers, respectively, were performed (Figure 4G). Based on the lack of any significant correlation, the changes in soluble parameters seem not to solely reflect differences in the T-cell infiltrate, and may instead represent specific immune cell activation.

Detection of spatially restricted patterns of immune activation induced by the DART

To facilitate the analysis of spatial differences in immune activation, it was next assessed whether the induction of immune responses by the DART could be detected by digital image analysis of immune activation markers. As the detection of soluble factors by immunohistochemistry is challenging, 13 markers of immune activation that are expressed either on the cell surface or in the nucleus were assessed (Figure 5A). These markers related to cytotoxicity (granzyme B, perforin, Tia1), proliferation (Ki67), interferon signalling (STAT1, IRF1, IRF5), apoptosis (caspase 3, caspase 9, APAF1) and immune checkpoint molecules (PD-1 and PD-L1); in addition, EpCAM was assessed as a marker for cancer cells (Figure 5B; Figure S5A, see online supplementary material). Notably, ex-vivo treatment with the DART induced upregulation of all cytotoxicity markers, as well as a strong increase in STAT1, in line with the secretion of IFNγ by all tumours (Figure 5C). These changes were accompanied by a decrease in EpCAM+ cancer cells, which may reflect killing of these cells by cytotoxic T cells. In addition, a trend towards higher PD-L1 expression was observed in some tumours, which is in line with the role of IFNγ as an inducer of PD-L1 expression.

To understand whether this technology would enable the detection of spatial differences in immune cell activation, a deep neural network was trained to automatically detect and localize tumour and stroma regions in each fragment (Figure 5D). While tumour and stromal content were comparable between conditions, the tumour regions were small (0.07 and 0.02 mm^2, on average, for untreated and DART-treated conditions, respectively), which resulted in a limited number of data points that could be analysed for the majority of markers (Figure S5B, see online

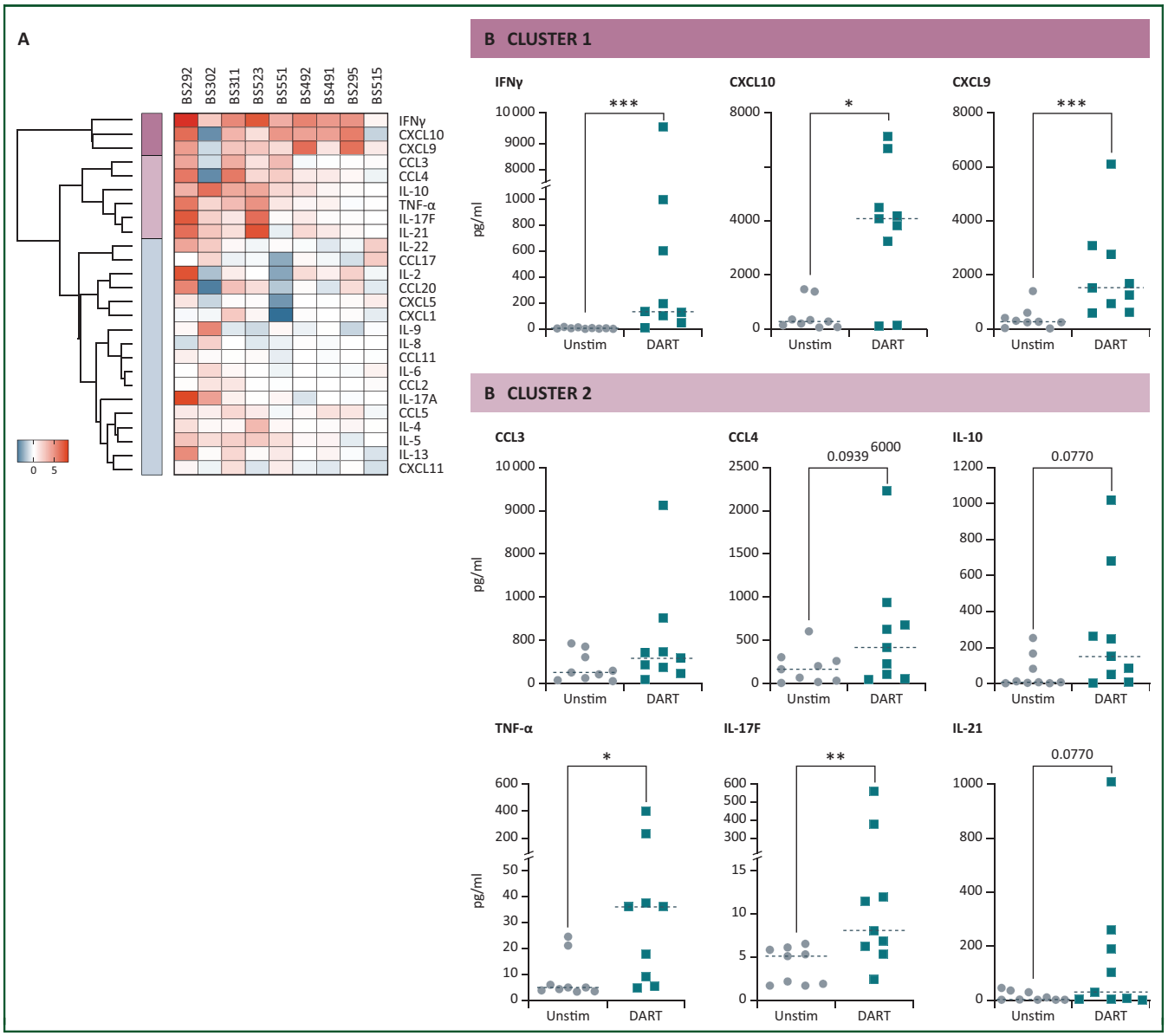

Figure 3. Cytokine and chemokine responses induced by the DART.
(A) Heatmap showing the log2-fold change for each of the 26 cytokines and chemokines analysed between the DART-treated and untreated condition (n=9 tumours, pooled analysis from the same experiment as shown in Figure 2). (B) Quantification of each cytokine or chemokine based on the clusters observed in Figure 2A. *P<0.05, **P<0.01, ***P<0.001 by two-tailed Mann–Whitney test.

supplementary material). Therefore, an exploratory analysis of six PDTFs from four tumours was performed, and markers for cytotoxicity, proliferation and interferon signalling in each region were quantified (Figure 5E,F; Figure S5C, see online supplementary material). This analysis showed a trend for the DART towards inducing cytotoxicity markers preferentially in T cells located in tumour regions (Figure 5F), which is in line with its design to activate T cells only when they are located in proximity to a FOLR1-expressing cell. This was not the case for the induction of Ki67 and STAT1, which were upregulated in both tumour and stroma regions. Notably, cells with a strong STAT1 signal (STAT1 2+/3+) were preferentially located in the stroma (Figure 5F). As STAT1 may indicate the presence of IFNγ-responsive cells, this observation suggests that the activation of T cells in tumour regions may be able to induce a broader immune response in surrounding stromal regions. Collectively, this initial data points to the potential of *iPROFILER* to measure local differences in cell-type-specific activation patterns at the tumour site.

DISCUSSION

While better patient stratification and the development of personalized immunotherapy treatments have become a central goal in immuno-oncology, our understanding of how such therapies act at the tumour site is still limited. Anti-tumour immune responses are dynamic multifaceted

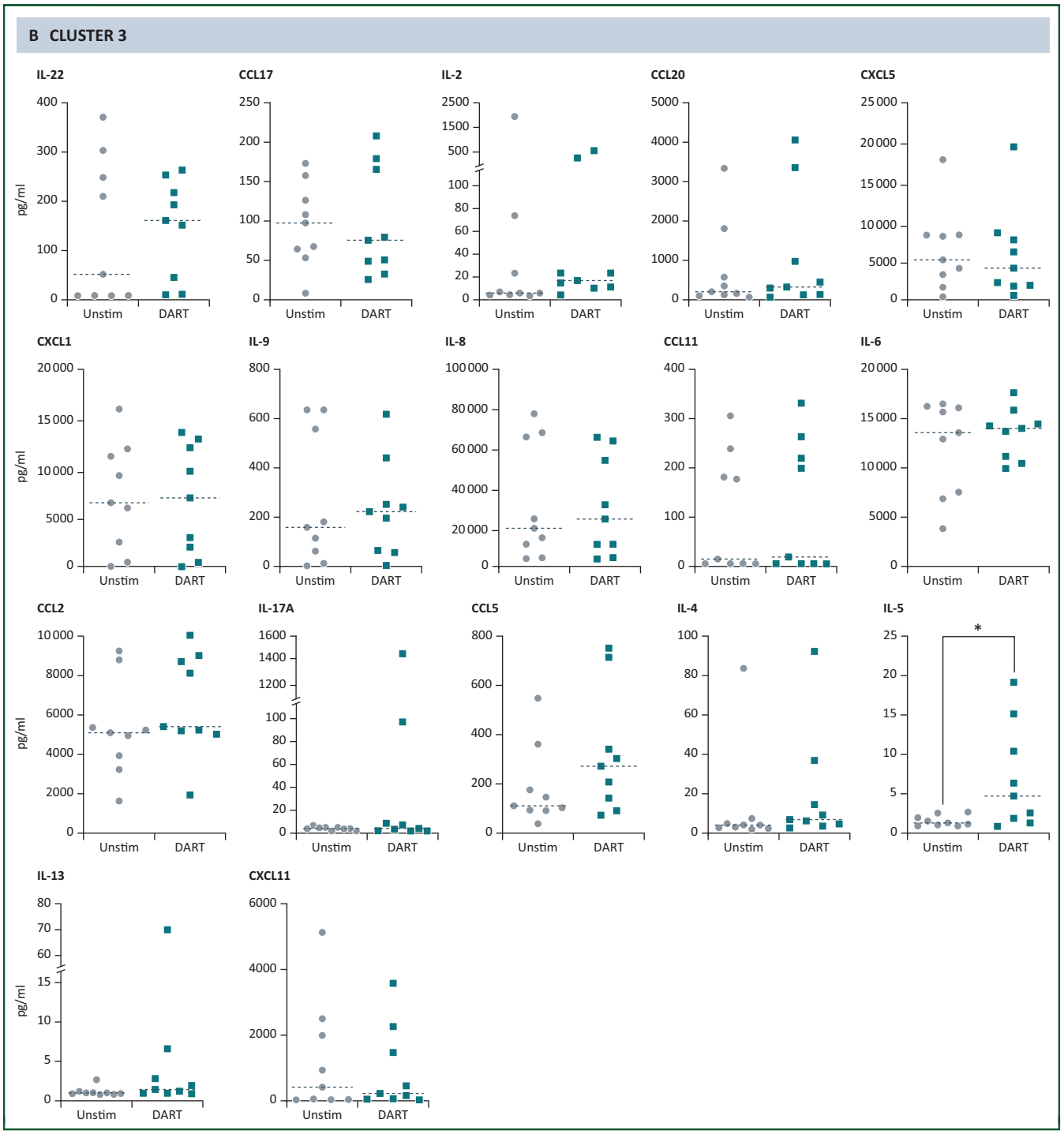

Figure 3. **Continued.**

processes that develop in heterogeneous TMEs, which makes it challenging to capture them within a single platform. Hence, technologies that can profile both the composition and architecture of the TME, as well as broad changes in immune activity upon treatment are crucial to gain a deeper understanding of how such immune responses develop.[17-19] This study describes the *iPROFILER* platform, which, by integrating multidimensional readouts in a flexible and modular manner, allows combined assessment of dynamic and spatial properties of treatment-induced immune responses in human cancer samples.

To establish the platform, a bifunctional FOLR1xCD3 DART was used as a tool for broad intratumoural T-cell stimulation.[13] As the DART does not depend on the presence of tumour-specific T cells, even a small number of tumour specimens is sufficient to capture T-cell activation, compared with, for instance, PD-1 blockade where T-cell reinvigoration is limited to a small group of patients.[20] In line with this

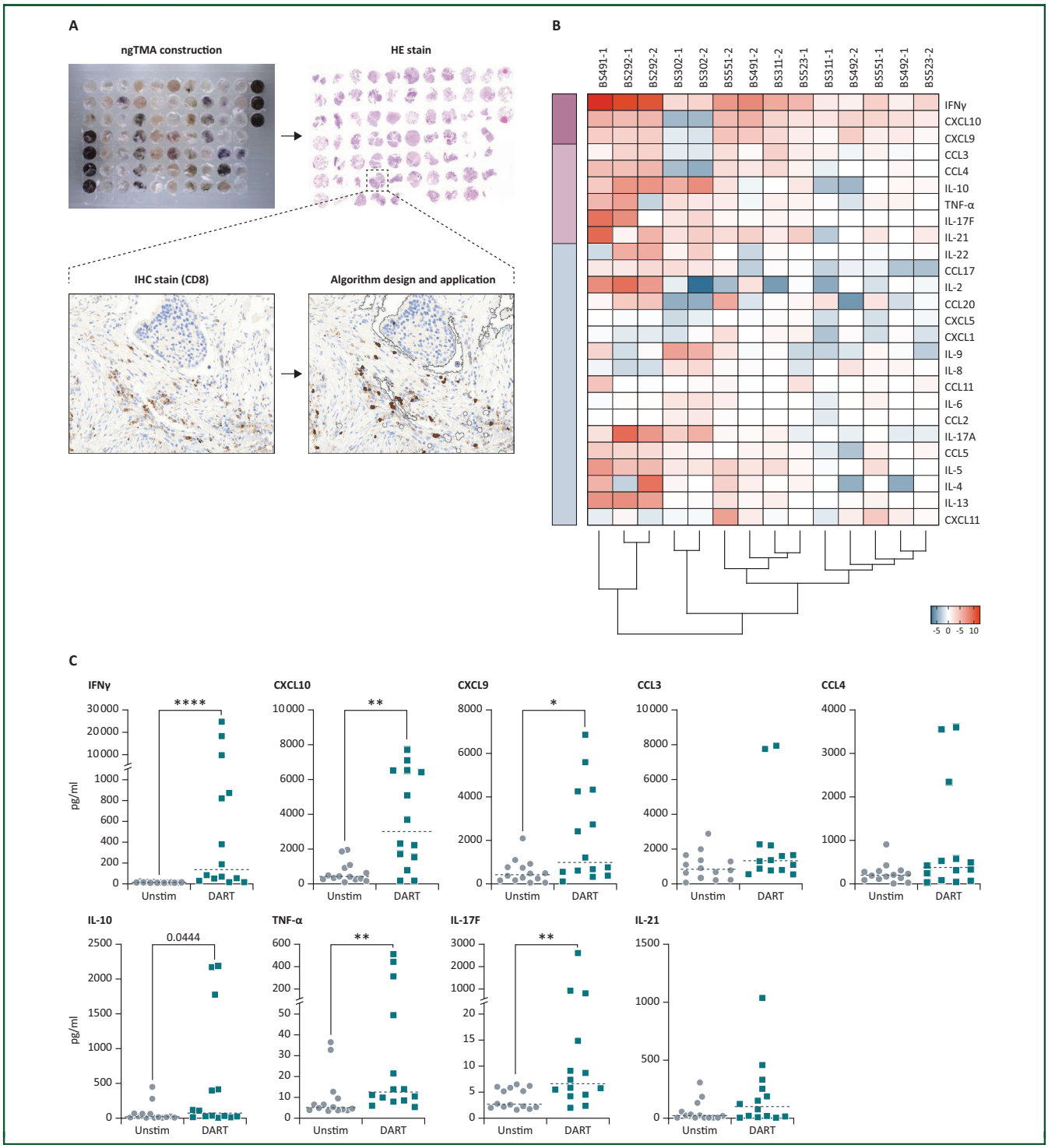

Figure 4. Development of an image analysis platform to visualize immune responses at single-cell level.
(A) Next-generation tissue microarray construction and digital image analysis pipeline. Patient-derived tumour fragments (PDTFs) from multiple experiments were arrayed on a single tissue block using a semi-robotic tissue microarrayer. Strict serial sections were cut and immunostained for cell lineage and activation markers, scanned at high resolution and analysed by digital image analysis. An example for a digital CD8 stain is shown (left). Image analysis is performed, and marker-positive cells are quantified per mm^2 tissue areas at single-cell resolution. Coloured mark-ups are generated for pathologist review and quality control (right). Pigment and glass background are automatically excluded from the analysis. (B) Heatmap showing the log2-fold change for each of the 26 cytokines and chemokines analysed between the DART-treated and untreated condition (n=7 tumours). Analysis of two individual tumour fragments are shown for each tumour. (C) Quantification of the most significant cytokines or chemokines related to clusters 1 and 2 in Figure 2A. (D) Correlation of the log2-fold changes of each soluble parameter between PDTFs assessed either in the flow cohort or in the immunohistochemistry (IHC) cohort. (E) Digital quantification of CD4+, CD8+ and FOXP3+ positive T cells and CD19+ B cells in unstimulated and DART-treated PDTFs. The algorithm is optimized for recognition and quantification of marker-positive lymphocytes (shown in brown) per mm^2 of tissue sample. (F) Quantification of CD4+, CD8+, FOXP3+ and CD19+ cells by IHC in the same tumours as in (B). (G) Spearman correlations between either CD4 or CD8 numbers and the expression of each cytokine or chemokine. *P<0.05, **P<0.01, ****P<0.0001 by two-tailed Mann—Whitney test in C and F.

https://doi.org/10.1016/j.iotech.2021.100034

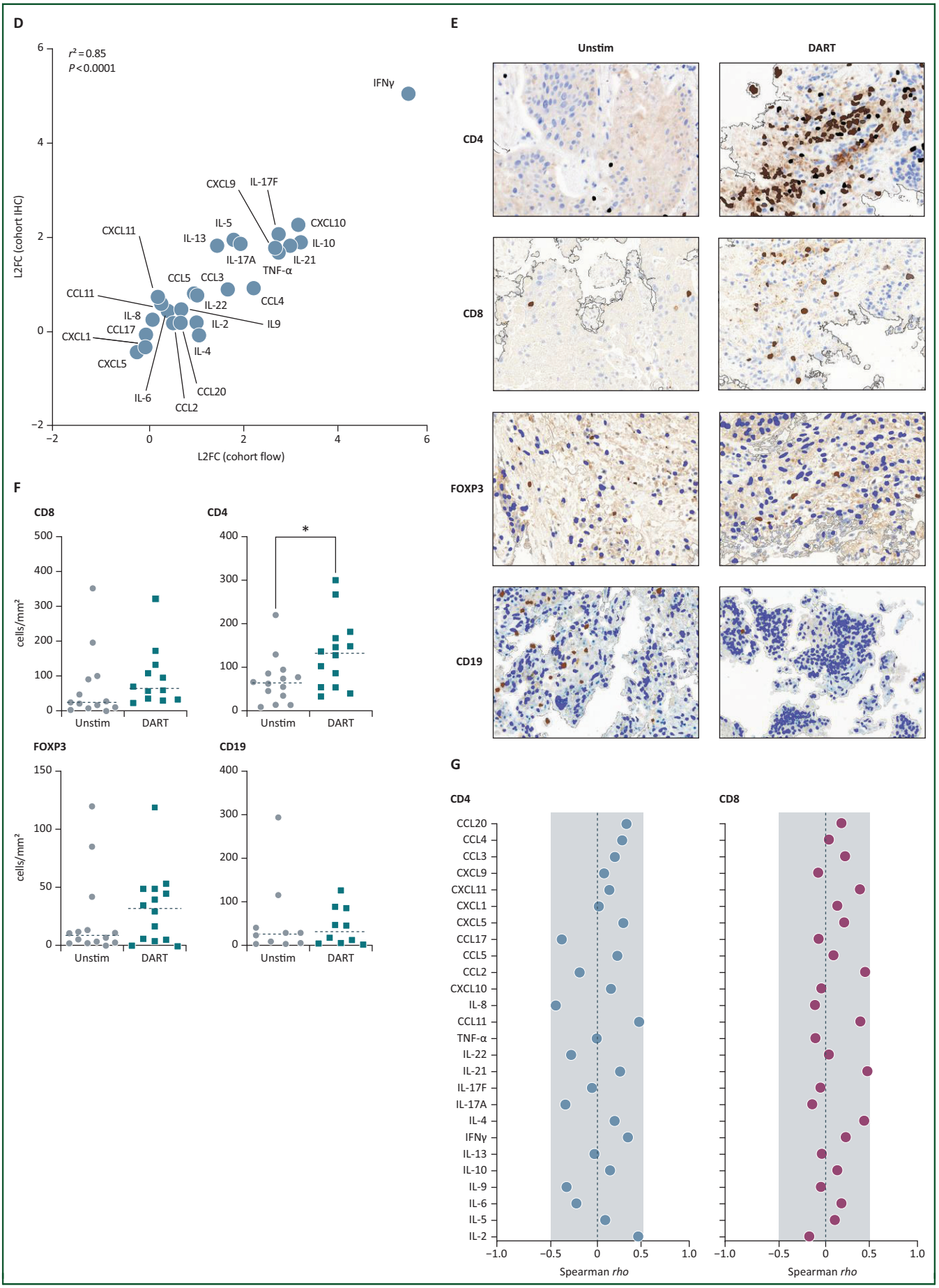

Figure 4. Continued.

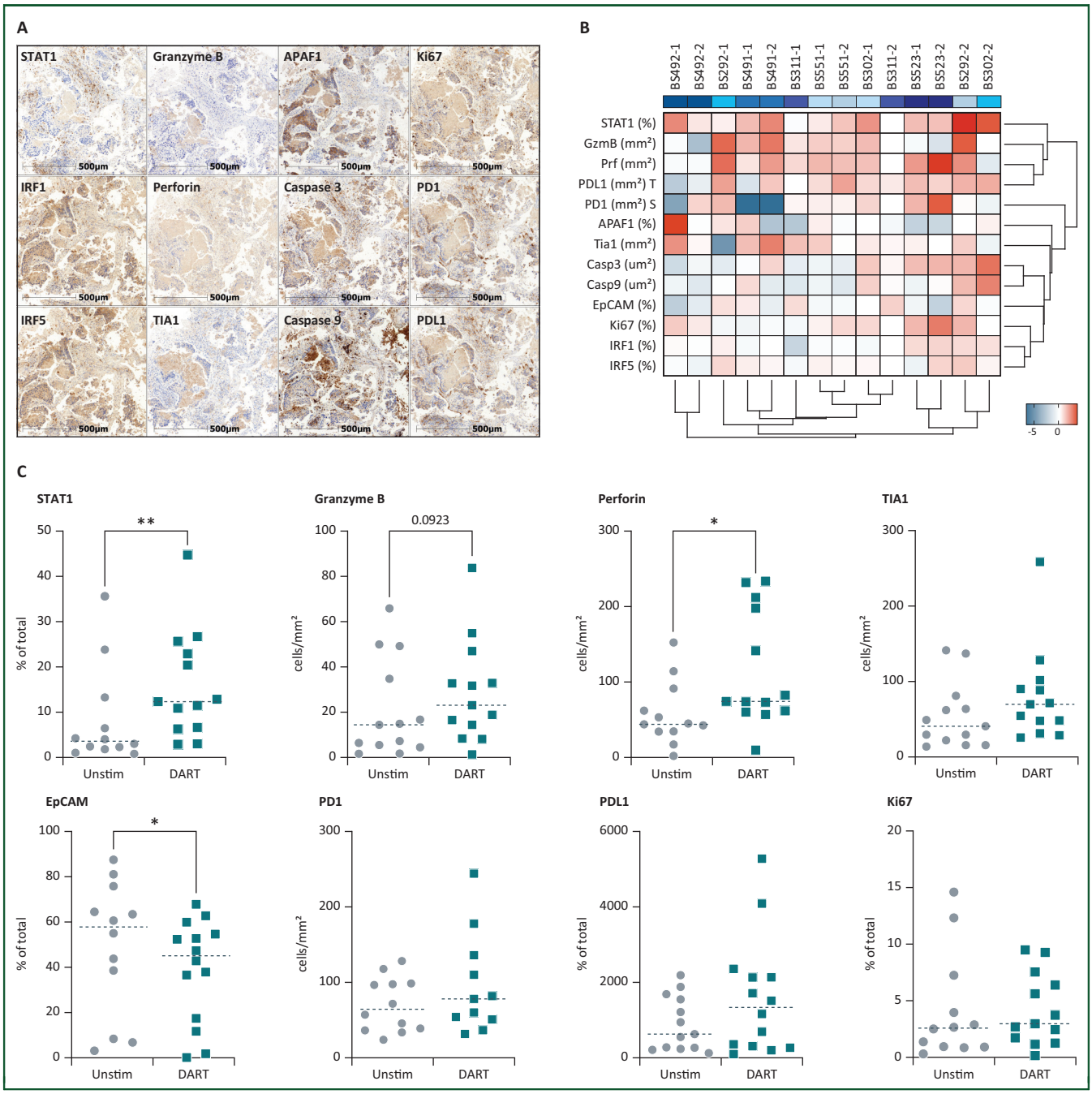

Figure 5. Immune activation and spatial immune response patterns following DART stimulation.
(A) Histology images from a DART-treated patient-derived tumour fragment (PDTF) showing expression of the interferon signalling molecules STAT1, IRF1 and IRF5 (first column); markers of cytotoxic T-cell activation (second column); and markers related to apoptosis (third column), proliferation (fourth column, top) and immune checkpoint expression (fourth column, middle and bottom). (B) Heatmap showing the log2 fold change for each of the 13 immune activation parameters analysed between the DART-treated and untreated condition by immunohistochemistry (n=7 tumours). Analysis of two individual tumour fragments are shown for each tumour. (C) Quantification of the most significantly changed immune activation markers (remaining markers are shown in Figure S5A, see online supplementary material). *P<0.05, **P<0.01 by two-tailed Mann—Whitney test. (D) Example of the tissue classification and cell quantification algorithms used to analyse lineage and immune activation markers (blue) in spatially segregated tumour (red) and stromal (green) areas. (E+F) Heatmap showing the log2-fold change (F) and quantification (G) of the indicated parameters separately for tumour and stromal areas in six individual PDTFs.

notion, after 48 h of ex-vivo treatment, an upregulation of activation markers on tumour-resident T cells, as well as release of inflammatory mediators dominated by an IFNγ-driven response was observed in samples expressing FOLR1. Of note, these changes are accompanied by an increase in T-cell numbers as well as in the expression of cytotoxic effector molecules. By applying digital image analysis and machine learning methods to segregate tumour and stromal regions, it was seen that T-cell activation seemed to predominantly occur in tumour areas, whereas the IFNγ-driven downstream responses showed the strongest signal in the stroma. Interestingly, two samples could be identified as non-/weak responders to the DART based on the lack of changes in immune activity. The platform further allowed

https://doi.org/10.1016/j.iotech.2021.100034

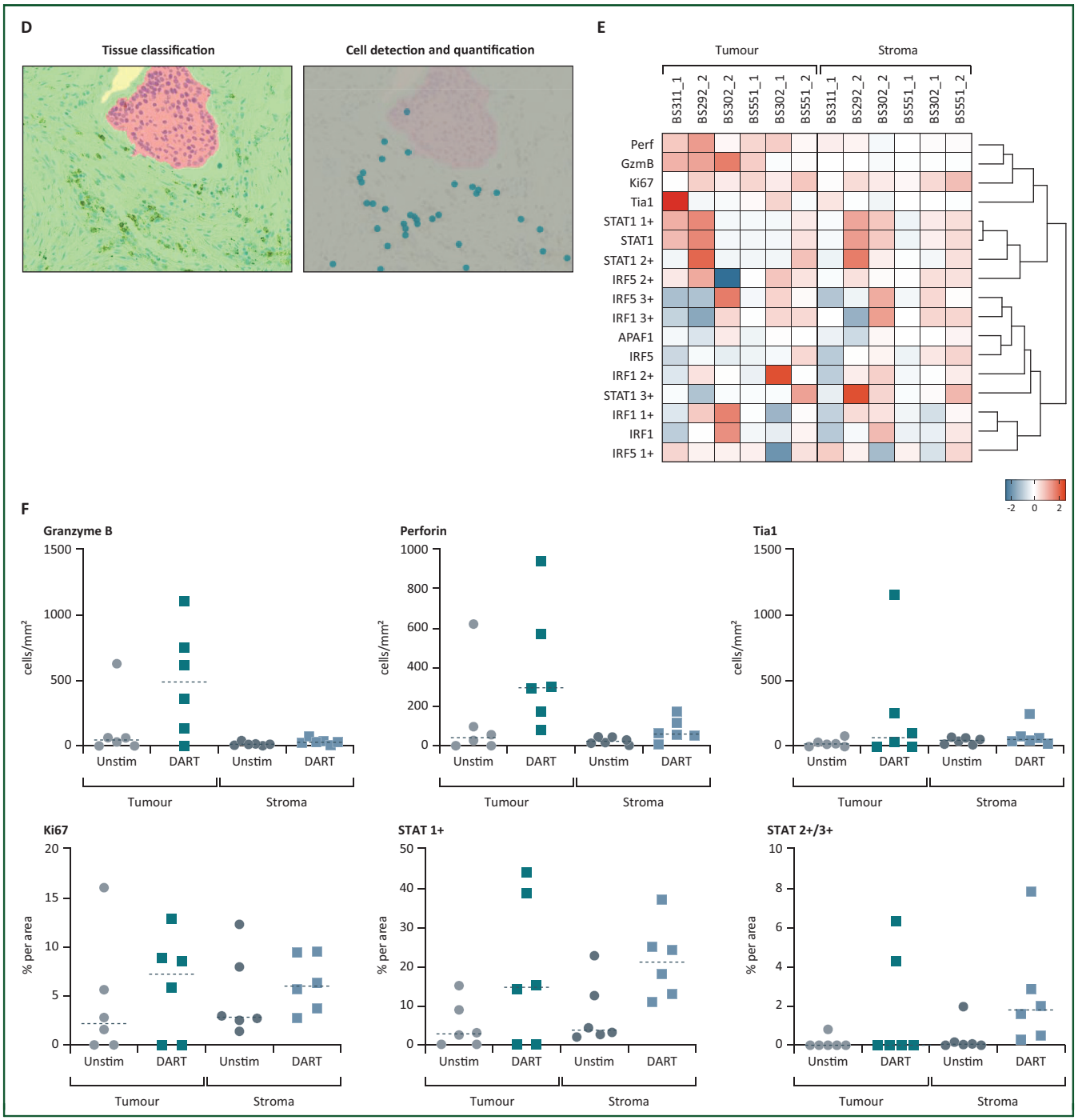

Figure 5. **Continued.**

delineation of low expression of FOLR1 and a lack of immune infiltrate as potential reasons for the lack of efficacy. Jointly, these data show that approaches such as the *iPROFILER* platform are capable of visualizing treatment-induced spatial and temporal alterations in the TME, which should help to gain new mechanistic insights into the development of immune responses at the tumour site. Moreover, such platforms can allow the identification of non-responding patients as well as potential underlying causes of resistance, which could facilitate the development of novel treatments, as suggested recently in the context of neoadjuvant immunotherapy combination trials in melanoma.[19]

This study reports a model system that, by preserving the cellular diversity and spatial interactions between tumour, stromal and immune populations, enables the dissection of in-situ immune responses after immunotherapeutic perturbations. As this was a proof-of-concept study, it is noted that the *iPROFILER* platform in its current form still has some limitations that may be optimized in future studies. First, to account for intratumour heterogeneity, some tumours may require a high number of tumour fragments. In this study, two to three PDTFs were used per condition, which was sufficient for a treatment such as the DART, which can theoretically activate every T cell in proximity of a cancer cell expressing

the target antigen. However, for therapies such as PD-1 blockade that rely on the reactivation of low-frequency tumour-specific T cells, this is likely not sufficient. Second, the current small size of the PDTFs (1 mm^3) makes spatial analyses challenging, and leads to the drop-out of samples affected by changes in tissue morphology and viability that may be induced during tumour processing or ex-vivo culture. The use of larger fragments or slice culture systems, as well as adaptations of the culture time, may help to overcome these two issues. Finally, this study utilized robust single-colour chromogenic immunohistochemistry stains to visualize immune cell infiltrates and activation markers. While this strategy enables better validation of the assessed markers, particularly in samples with high inherent variability such as human tumour tissue, this may not be sufficient for the assessment of more complex changes in multiple immune cell populations. The ngTMA design, which reduces variability in staining and tissue analysis methods over standard methods, could support the combination of PDTF cultures with novel highly multiplexed imaging methods such as CODEX,[21] imaging mass cytometry[22] or spatial RNA sequencing[23] approaches. A core strength of the *iPROFILER* platform lies in the strict spatial correspondence of the tissue samples utilized for functional and tissue-level analysis. Utilizing advanced bioinformatics methods and artificial intelligence for scientific discovery, integration of the *iPROFILER* platform with high-dimensional spatial readouts could provide novel insights into mechanistic interactions of immune, tumour and stromal cell populations that cannot otherwise be captured in clinical samples. Ultimately, results from such analyses should foster the identification of new biomarkers and the development of personalized immunotherapy treatments.

CONCLUSIONS

This article describes a proof-of-principle study utilizing the ex-vivo PDTF platform for in-depth profiling of the in-situ immune response to immunostimulatory drugs in patient samples. By integrating functional assays and spatial analysis, this platform can provide an in-depth analysis of the immune contexture linked to response and non-response to immuno-oncology drugs. This approach could be of great clinical utility to develop personalized immunotherapy treatments while, at the same time, providing ample opportunities for exploratory science to improve our biological understanding of disease.

ACKNOWLEDGEMENTS

The authors wish to thank Melanie Sachs, the team of the DBM flow facility, and the team of the Translational Research Unit at the Institute of Pathology, University of Bern for outstanding technical assistance, and Dr. Spasenija Savic for assistance with acquisition of patient tissue samples.

FUNDING

This work was supported by the Swiss National Science Foundation (Grants P2SKP3_168322/1 and P2SKP3_168322/2 to V. H. K., 320030_188576/1 to A. Z. and P300PB_164755 to D. S. T), the Promedica Foundation F-87701-41-01 (to V. H. K), the Edoardo R., Giovanni, Giuseppe and Chiarina Sassella Foundation (to D. S. T.), and the Research Funds of the University of Basel (to D. S. T.). C. R. acknowledges funding by NIH Grant R01 CA181258.

DISCLOSURE

V. H. K. has served as an invited speaker on behalf of Indica Labs. All other authors declare no conflicts of interest.

SUPPLEMENTARY DATA

Supplementary data to this article can be found online at https://doi.org/10.1016/j.iotech.2021.100034.

REFERENCES

1. Ribas A, Wolchok JD. Cancer immunotherapy using checkpoint blockade. *Science*. 2018;359:1350-1355.
2. Robert C. A decade of immune-checkpoint inhibitors in cancer therapy. *Nat Commun*. 2020;11:3801.
3. Kalbasi A, Ribas A. Tumour-intrinsic resistance to immune checkpoint blockade. *Nat Rev Immunol*. 2020;20:25-39.
4. Wolchok JD, Chiarion-Sileni V, Gonzalez R, et al. Overall survival with combined nivolumab and ipilimumab in advanced melanoma. *N Engl J Med*. 2017;377:1345-1356.
5. Hellmann MD, Paz-Ares L, Bernabe Caro R, et al. Nivolumab plus ipilimumab in advanced non-small-cell lung cancer. *N Engl J Med*. 2019;381:2020-2031.
6. Motzer RJ, Tannir NM, McDermott DF, et al. Nivolumab plus ipilimumab versus sunitinib in advanced renal-cell carcinoma. *N Engl J Med*. 2018;378:1277-1290.
7. Xin Yu J, Hodge JP, Oliva C, et al. Trends in clinical development for PD-1/PD-L1 inhibitors. *Nat Rev Drug Discov*. 2020;19:163-164.
8. Murciano-Goroff YR, Warner AB, Wolchok JD. The future of cancer immunotherapy: microenvironment-targeting combinations. *Cell Res*. 2020;30:507-519.
9. Voabil P, de Bruijn M, Roelofsen LM, et al. An ex vivo tumor fragment platform to dissect response to PD-1 blockade in cancer. *Nat Med*. 2021. https://doi.org/10.1038/s41591-021-01398-3.
10. Koelzer VH, Sirinukunwattana K, Rittscher J, Mertz KD. Precision immunoprofiling by image analysis and artificial intelligence. *Virchows Arch*. 2019;474:511-522.
11. Zlobec I, Koelzer VH, Dawson H, et al. Next-generation tissue microarray (ngTMA) increases the quality of biomarker studies: an example using CD3, CD8, and CD45RO in the tumor microenvironment of six different solid tumor types. *J Transl Med*. 2013;11:104.
12. Simonyan K, Zisserman A. Very Deep Convolutional Networks for Large-Scale Image Recognition. arXiv:1409.1556v6 [cs.CV] 2015.
13. Rader C. Bispecific antibodies in cancer immunotherapy. *Curr Opin Biotechnol*. 2020;65:9-16.
14. Schreiner J, Thommen DS, Herzig P, et al. Expression of inhibitory receptors on intratumoral T cells modulates the activity of a T cell-bispecific antibody targeting folate receptor. *Oncoimmunology*. 2016;5:e1062969.
15. Walseng E, Nelson CG, Qi J, et al. Chemically programmed bispecific antibodies in diabody format. *J Biol Chem*. 2016;291:19661-19673.
16. Xia W, Low PS. Folate-targeted therapies for cancer. *J Med Chem*. 2010;53:6811-6824.
17. Models for Immuno-oncology Research. *Cancer Cell*. 2020;38:145-147.
18. Politi K. Leveraging patient-derived models for immunotherapy research. *Am Soc Clin Oncol Educ Book*. 2020;40:e344-e350.
19. Versluis JM, Thommen DS, Blank CU. Rationalizing the pathway to personalized neoadjuvant immunotherapy: the Lombard Street Approach. *J Immunother Cancer*. 2020;8:e001352.

20. Peters S, Kerr KM, Stahel R. PD-1 blockade in advanced NSCLC: a focus on pembrolizumab. *Cancer Treat Rev.* 2018;62:39-49.
21. Schurch CM, Bhate SS, Barlow GL, et al. Coordinated cellular neighborhoods orchestrate antitumoral immunity at the colorectal cancer invasive front. *Cell*. 2020;183:838.
22. Giesen C, Wang HA, Schapiro D, et al. Highly multiplexed imaging of tumor tissues with subcellular resolution by mass cytometry. *Nat Methods*. 2014;11:417-422.
23. Method of the year 2020: spatially resolved transcriptomics. *Nat Methods*. 2021;18:1.